The Company of **Biologists**

RESEARCH REPORT

Control of patterns of symmetric cell division in the epidermal and cortical tissues of the *Arabidopsis* root

Yanwen Zhang, Michail Iakovidis* and Silvia Costa‡

ABSTRACT

Controlled cell division is central to the growth and development of all multicellular organisms. Within the proliferating zone of the *Arabidopsis* root, regular symmetric divisions give rise to patterns of parallel files of cells, the genetic basis of which remains unclear. We found that genotypes impaired in the *TONNEAU1a* (*TON1a*) gene display misoriented symmetric divisions in the epidermis and have no division defects in the underlying cortical tissue. The *TON1a* gene encodes a microtubule-associated protein. We show that in the *ton1a* mutant, epidermal and cortical cells do not form narrow, ring-like preprophase bands (PPBs), which are plant-specific, cytoskeletal structures that predict the position of the division plane before mitosis. The results indicate that in the cortex but not in the epidermis, division plane positioning and patterning can proceed correctly in the absence of both a functional *TON1a* and PPB formation. Differences between tissues in how they respond to the signals that guide symmetric division orientation during patterning might provide the basis for organised organ growth in the absence of cell movements.

KEY WORDS: Tissue patterning, *TON1a*, Meristem, Epidermis, Cortex, Preprophase band

INTRODUCTION

In plants, where the presence of cell walls prevents cell movement, pattern formation studies can provide insights on how the control of cell division orientation leads to tissue and organ organisation. The *Arabidopsis* root is a simple system to investigate symmetric division control because perturbations in division patterns can be easily observed. In the root meristem, the zone where cells proliferate, the different cell types originate by asymmetric divisions from sets of stem cells. Subsequently, each cell population is expanded through regular, symmetric divisions, resulting in an organ composed of mono-layered tissues organised concentrically. During symmetric division in the epidermis and in the underlying cortical tissue, cells position their division plane in an anticlinal, transverse orientation and form a regular pattern of parallel files of cells arranged along the proximodistal axis of the root (Fig. 1A-C) (Dolan et al., 1993).

The preprophase band (PPB) is a transient array of microtubules that forms a narrow ring underneath the cell membrane during the G2 phase of the cell cycle and marks precisely the position of the

Department of Cell and Developmental Biology, John Innes Centre, Norwich NR4 7UH, UK.
*Present address: Department of Biology, University of North Carolina, Chapel Hill, NC, USA.

‡Author for correspondence (s.costa2537@gmail.com)

division plane in the M phase. Mutant and drug studies suggest a crucial role for the PPB in the control of division plane orientation (Rasmussen et al., 2011, 2013). However, the few identified *Arabidopsis* mutants that are unable to form PPBs – the loss-of-function *tonneau1* (*ton1*) and *fass* (also known as *ton2*) – have impaired organisation of interphase microtubules, severe pleiotropic defects and extremely short roots where the regular division patterns are disrupted (Azimzadeh et al., 2008; Camilleri et al., 2002; Torres-Ruiz and Jurgens, 1994; Traas et al., 1995) and cannot provide information on cell division control at the tissue level. Here, we sought to identify the genetic basis of the pattern of epidermal and cortical symmetric divisions in the *Arabidopsis* root.

RESULTS AND DISCUSSION

Through a forward genetic screen we isolated the recessive *nomad* (*nom*) mutant (see supplementary Materials and Methods). In the epidermis of WT roots, 98.84% of the symmetric divisions are in a transverse orientation relative to the proximodistal axis of the root, whereas in *nom*, only 51.13% are transverse and the other 48.87% are oblique (Fig. 1B,F,J). In the cortical tissue, cells divide again in a transverse orientation in the wild type (WT) and this is unchanged in *nom* (Fig. 1C,G). The concentric organisation of root tissues and the organisation of the stem cells niche reflect the ability of the stem cells to divide asymmetrically and to give rise to the different tissue types (Dolan et al., 1993), and they are the same in *nom* and WT (Fig. 1D,H,E,I). In *nom*, some defects in division orientation can been seen in the endodermis, the tissue subtending the cortex (Fig. 1D,H); however, division patterns along the root-hypocotyl axis during embryonic development are unaltered (Fig. S1). This indicates that the *nom* mutation alters the orientation of the symmetric divisions, but does not affect the root asymmetric divisions in the seedlings or the regular division patterns during embryogenesis.

Mutant *nom* seedlings can be discriminated from WT seedlings at 4 days post germination (dpg) by a small reduction in root length, which becomes more pronounced at 8 dpg (Fig. 1K,L), but along the proximodistal axis of the root, the meristem size of *nom* is unchanged compared with that of the WT (Fig. 1M). Within the radial dimension, 8 dpg *nom* root meristems were 20% wider than the WT (Fig. 1D,H,N). Although tissues were also mono-layered in the *nom* epidermis, they had 58.5% more cells than in the WT; by contrast, the increase in cell numbers was not as great in the *nom* cortex compared with the WT (+18%; Fig. 1,O). As division orientation determines to which growth axis of the organ the new cell will contribute, such a difference in epidermal cell number can be correlated with the oblique orientation of *nom* epidermal divisions.

The *nom* mutation was mapped to the *TON1a* (At3g55000) locus (Fig. 2A). Complementation with a genomic fragment that restores the *nom* phenotype to WT (Fig. 2B,C) and the identification of two recessive, T-DNA insertion alleles, *ton1a-2*
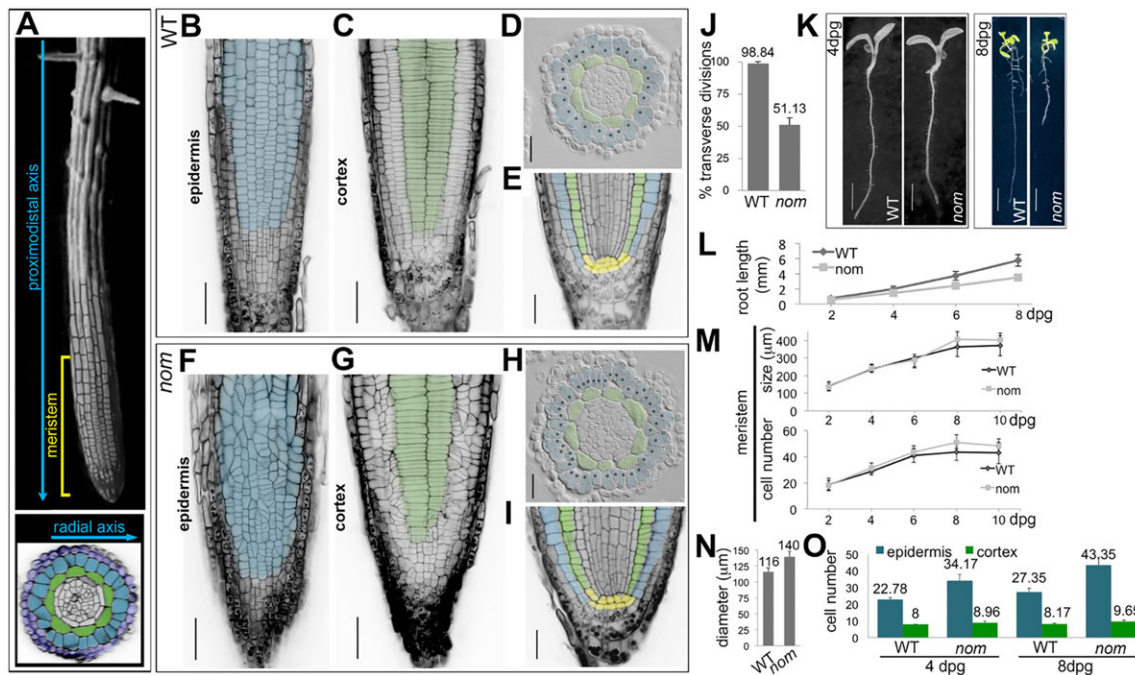
DEVELOPMENT

Fig. 1. The *nom* mutation affects the patterns of symmetric cell divisions in the *Arabidopsis* root meristem epidermis but not in the underlying cortical tissue. (A) Top, SEM image of an *Arabidopsis* root with a superimposed confocal image of the root epidermis in the meristem; bottom, radial organisation of the root in a transverse section in the meristem: the epidermis (in blue) overlays the cortical tissue (in green) and on the outside is surrounded by the lateral root cap tissue (in dark blue). (B-I) Organisation of the root meristem in WT and *nom* mutant seedlings at 8 dpg. Note that in plants, the orientation of the cell walls, highlighted in black by propidium iodide (PI) staining, reflects the orientation of the division planes. Epidermal cells are pseudocoloured in blue, cortical cells in green. (B,C,F,G) Cellular organisation and division plane orientation in the epidermis and underlying cortical layer, images are single, longitudinal confocal sections of Schiff-PI stained meristems. Scale bars: 50 μm. (D,H) Transverse sections in the root meristem of resin-embedded seedlings; each black dot marks a single epidermal cell. Scale bars: 25 μm. (E,I) Single, median-longitudinal confocal sections in Schiff-PI-stained root meristems; stem cell niche are pseudocoloured in yellow. Scale bars: 25 μm. (J) percentage of transverse divisions in the root, meristematic epidermis of 8 dpg seedlings; WT *n*=19, *nom n*=20. (K) Whole seedlings at 4 and 8 dpg. Scale bars: 2 mm and 7.5 mm, respectively. (L-N) Data quantification. Root length (L) and meristem size (M) measured over time; for each time point, WT *n*=58, *nom n*=58 (L), WT *n*=40, *nom n*=40 (M); (N) diameter of the meristem; WT *n*=23, *nom n*=26; (O) number of epidermal and cortical cells scored in transverse sections within the root meristem at 4 and 8 dpg; at 4 dpg, WT *n*=319 epidermal and 113 cortical cells in 14 roots, *nom n*=786 epidermal and 206 cortical cells in 23 roots; at 8 dpg, WT *n*=629 epidermal and 188 cortical cells in 23 roots, *nom n*=1127 epidermal and 251 cortical cells in 26 roots. All data are means±s.d.; mean values are shown above bars for J,N,O.

(GK-016D04) and *ton1a-3* (GK-727H06), which display epidermal-specific division defects like *nom*, confirmed its identity (Fig. 2D). The *nom* allele was renamed *ton1a-1*. *TON1a* lies in tandem to *TON1b*; they encode proteins that are 85% identical at the amino acid level and the two genes have been proposed to function redundantly (Azimzadeh et al., 2008). However, more recently, a unique function for the *TON1a* gene was hypothesised from biochemical studies (Spinner et al., 2013) and from a genetic interaction found between a *fass/ton2-15* allele and the *ton1a-te500* allele that has a WT root phenotype (Kirik et al., 2012). Our RT-PCR analysis shows that in the roots of the *ton1a-1*, *ton1a-2* and *ton1a-3* alleles there is a severe reduction in the *TON1a* transcript compared with that in WT roots and the *TON1b* gene is expressed as normal (Fig. 2E-G). This suggests that the consistent mutant phenotype we observed in the three *ton1a* alleles is caused by a reduction in the *TON1a* transcript and that the three *ton1a* alleles are hypomorphic alleles of *TON1a*. Thus, our data show the first direct, genetic evidence of a requirement for a functional *TON1a* gene alone in the control of symmetric division orientation within the root epidermis, but not in the underlying cortical tissue.

To test whether the root epidermal and cortical cells in *ton1a-1* form PPBs, we used anti-α-tubulin immunolocalisation. The narrow PPB ring of microtubules that forms at the cellular periphery can be seen as bright foci on each side of the cell in median confocal

sections within WT cells (Fig. 3A). Instead, in median confocal sections within *ton1a-1* cells of the epidermal and cortical tissues, or of the inner tissues, we did not detect any bright foci, or structures resembling it and only detected more pronounced labelling around the nuclear periphery (Fig. 3A; Fig. S2), like in the studies of the loss-of-function *ton1* and *fass* mutants (Azimzadeh et al., 2008; Camilleri et al., 2002; Traas et al., 1995). Later division structures (spindle and cytokinetic phragmoplast) were normal in *ton1a-1* compared with the WT (Fig. 3A). Only occasionally were PPBs seen in lateral root cap cells, which surround the epidermis (data not shown). The absence of PPB formation in the epidermis and cortex was confirmed by examining *in vivo* the expression of the microtubule marker RFP-TUA5 in the *ton1a-1* mutant (Fig. 3B). Also, we were unable to detect PPBs in *ton1a-1* epidermal cells by *in vivo* time-course imaging using GFP-β-tubulin (Fig. 3C). Thus, *TON1a* appears consistently necessary to form the narrow PPBs in both the epidermis and the cortex, yet division orientation is correctly in place in the cortex, but not in the epidermis. Such ability of cells in the cortex to divide correctly is consistent with studies on cell cultures that have shown division plane can also be correctly placed without the formation of narrow PPBs (Chan et al., 2005; Marcus et al., 2005) and with the observations that not all plant species or all cell types form PPBs (Pickett-Heaps et al., 1999; Rasmussen et al., 2013). This suggests that PPB-independent mechanisms can guide division plane positioning in organised tissues.
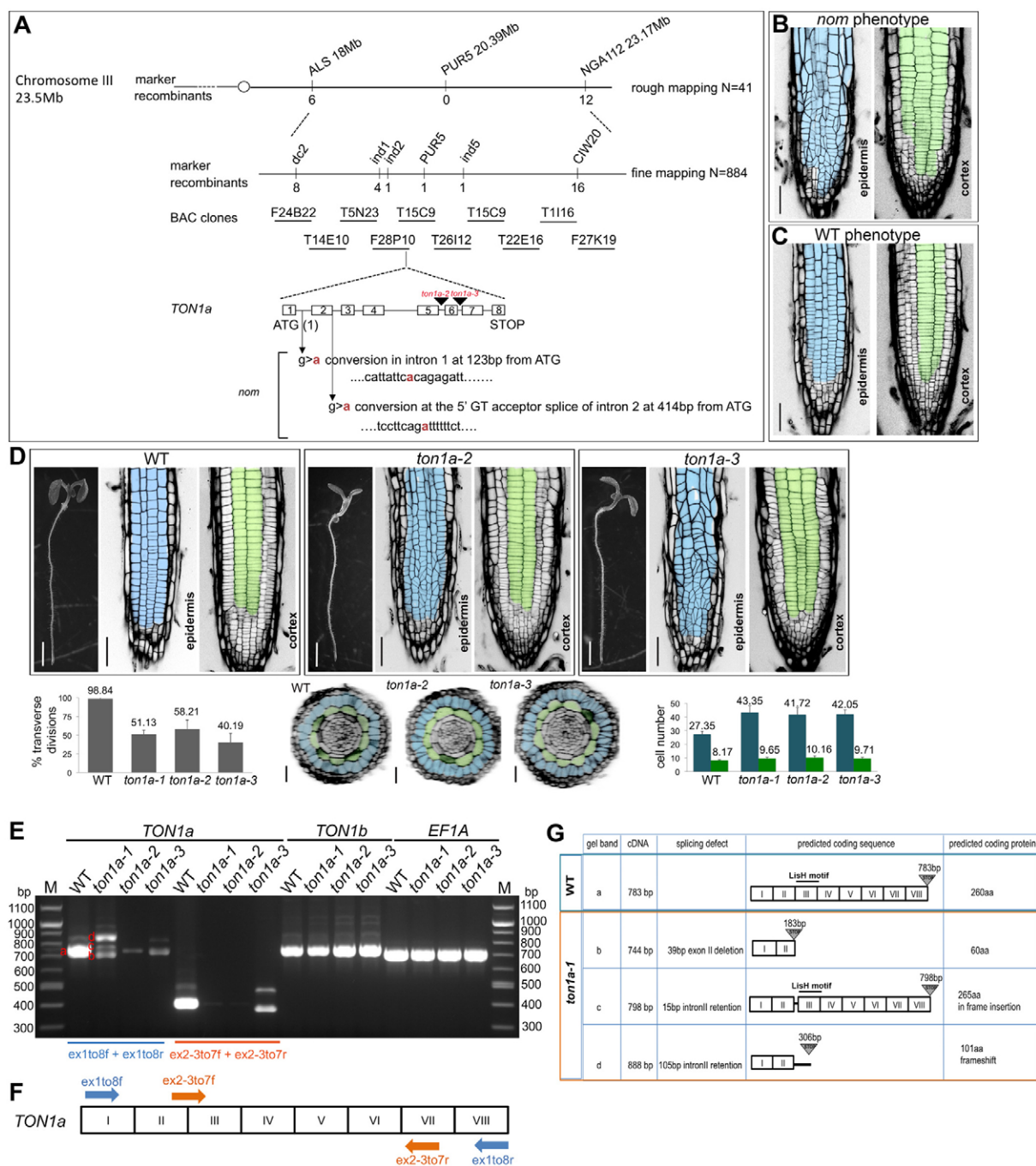
Fig. 2. The *nom* mutation maps to the *TON1a* gene and the three *ton1a* alleles identified are hypomorphic alleles of *TON1a*. (A) Genetic mapping delimited the *nom* mutation to BAC clone F28P10. Schematic representation of the organisation of the gene, position of the point mutations relative to the start codon and position of the T-DNA insertions in the *ton1a-2* and *ton1a-3* alleles; *nom* was later renamed as the *ton1a-1* allele. (B,C) Confocal images of 4 dpg T2 seedlings segregating *nom* and WT phenotypes from T1 BASTA-resistant *nom* plants carrying the complementing construct. Epidermis is pseudocoloured in blue, cortex in green. Scale bars: 50 μm. (D) Phenotypic characterisation of the *ton1a-2* and *ton1a-3* alleles. Stereomicroscope images of whole seedlings and confocal images of the epidermis and cortex in the root meristem of WT and *ton1a-2* and *ton1a-3* alleles at 4 dpg, quantification of epidermal transverse divisions at 8 dpg; WT *n*=19, *ton1a-2 n*=18, *ton1a-3 n*=21; reconstructed transverse sections and respective quantification of epidermal and cortical cell numbers at 8 dpg, including those calculated for the *ton1a-1* allele; WT *n*=629 epidermal and 188 cortical cells in 23 roots, *nom n*=1127 epidermal and 251 cortical cells in 26 roots, *ton1a-2 n*=751 epidermal and 183 cortical cells in 18 roots, *ton1a-3 n*=883 epidermal and 204 cortical cells in 21 roots. Data are means±s.d. Scale bars: 2 mm for all seedlings, 50 μm for epidermis and cortex and 25 μm for transverse sections. (E-G) Molecular characterisation of the three *ton1a* alleles. (E) RT-PCR analysis with primer pairs specific for *TON1a* ex1to8f/r (in blue) produces in the *ton1a-1* allele three main transcripts (indicated with red b,c,d letters), and in the *ton1a-2* and *ton1a-3* alleles produces a severe reduction in the *TON1a* transcript compared with the WT. The transcripts in *ton1a-1* were cloned and sequenced to confirm they resulted from mis-splicing. Primer pairs ex2-3to7f/r (in orange) amplify only the correctly spliced WT transcript of *TON1a* and produce consistently barely detectable WT transcript for the *ton1a-1* allele. As a loading control, primer pairs that amplify the elongation factor 1A (*EF1A*) were used. (F) Schematic representation of primer locations on the *TON1a* cDNA; exons are indicated by roman numerals. (G) Schematic summary of RT-PCR and cloning results with the predicted amino acid sequences resulting from the mis-splicing of *TON1a* transcript in the *ton1a-1* allele and the location of the LisH dimerisation motif.
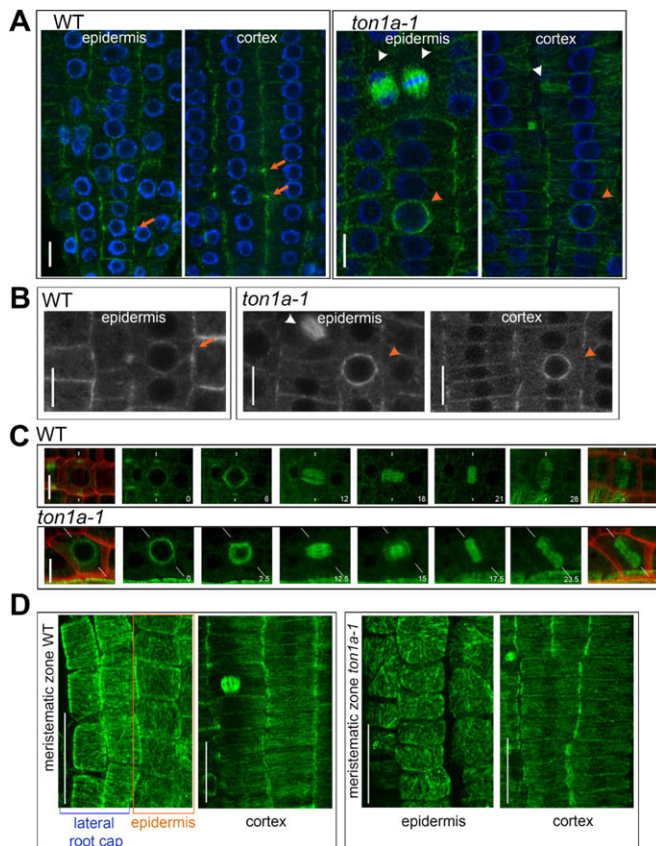
Fig. 3. In the root meristem, _TON1a_ is required to form PPBs in both the epidermis and the cortex but does not control the organisation of interphase microtubules, which differs between the two tissues. (A,B) Localisation of cytoskeletal structures in the meristematic epidermis of WT and _ton1a-1_ roots, PPB (orange arrows), abundant microtubules surrounding the nucleus (orange arrowheads), spindle and cytokinetic phragmoplast (white arrowheads); all images are single, confocal sections. (A) Roots immunostained with α-tubulin (green), nuclei are stained blue with DAPI; WT _n_=6 roots observed 13 PPBs in the epidermis and 23 PPBs in the cortex, _ton1a-1 n_=6 roots. (B) Representative close-up images of meristematic epidermal and cortical cells expressing _in vivo_ the tubulin marker RFP-TUA5 (grey); WT _n_=12 roots observed 37 PPBs in the epidermis and 48 PPBs in the cortex, _ton1a-1 n_=10 seedlings. (C) Stills from a confocal time-lapse movie of epidermal cells of WT and _ton1a-1_ seedlings expressing GFP-β-tubulin from G2 phase to the end of M-phase (left to right); time is indicated in minutes, maximum intensity projections of confocal _z_-series, in the first and last stills the GFP images have been merged with PI images (red) to outline the cell walls, the white lines indicate the position of the division plane. (D) Representative images of maximum intensity projections of confocal optical sections in the epidermis and cortex of WT and _tona1-1_ roots immunostained with α-tubulin (green); WT _n_=6, _ton1a-1 n_=6. Note that in the first panels, epidermal cells (framed within an orange outline) are present in the same projections as lateral root cap cells. Scale bars: 10 μm (A-C) and 25 μm (D).

The restriction of the defects in symmetric division orientation and patterning to the epidermal tissue in the three _ton1a_ mutant alleles we have characterised raises the question of how such a tissue-specific phenotype might emerge. _TON1a_ is part of the large TTP (TON1/TRM/PP2A) protein complex (Spinner et al., 2013). The possibility that mutations in _TON1a_ affect the interactions between TON1a and the other components of the TTP complex in a tissue-specific manner seems unlikely because _ton1a_ epidermal and cortical cells are equally unable to form narrow PPBs. An alternative possibility is that in the two tissues, cells have different requirements for a functional _TON1a_ gene and for the formation of the PPB in the

control of division plane orientation. We speculated whether the organisation of the interphase microtubules might underlie such different requirements. We found that, similar to what was also observed in WT meristems by Bichet et al. (2001), in both WT and _ton1a-1_ meristems the interphase microtubules are not organised in epidermal cells and instead have a prevalent transverse organisation in cortical cells, which is parallel to the correct orientation of the division plane (Fig. 3D; Fig. S3). This suggests that in root meristematic cells, the _TON1A_ gene is required for the formation of PPBs and not for the overall organisation of interphase microtubules. In addition, this result raises the possibility that the PPB might function to accurately fix division plane orientation in epidermal cells, where interphase microtubules and the cues responsible for division plane orientation are not aligned. Otherwise, where interphase microtubules are already aligned with such cues, PPB might be redundant, as seen in cortical cells. Such a possibility will need to be experimentally tested in further studies. Our results point to the existence of tissue-specific responses to the signals guiding the orientation of symmetric cell division during tissue patterning. This could be key to ensuring organised growth within proliferating meristems.

MATERIALS AND METHODS
Plant lines and growth conditions
The _Arabidopsis thaliana_ T-DNA insertion lines GK-727H06 (N469786), GK-016D04 (N401480) and the _GFP-TUB6_ line (N6550) were obtained from the Nottingham _Arabidopsis_ stock centre (NASC). Descriptions of the following lines have been published: _GL2::GUS_ (Masucci and Schiefelbein, 1996), GFP-MBD (Granger and Cyr, 2001) and RFP-TUA5 (Gutierrez et al., 2009). Phenotypic analysis was undertaken on _ton1a-1_ mutant seedlings backcrossed three times into the parental _GL2::GUS_ line. The _ton1a-1_ phenotype was always compared against the phenotype of the parental line _GL2::GUS_ (referred to here as WT). GK-727H06 (N469786) and GK-016D04 (N401480) T-DNA insertion lines were confirmed by PCR genotyping using primers listed in Table S1 as described in the supplementary Materials and Methods.

Seeds were surface sterilised in 10% sodium hypochlorite and sown on plates prepared with Murashige and Skoog (MS) salts (Duchefa), 1% sucrose and 0.5% phytagel (Sigma) medium (pH 5.8). Seeds were stratified in the dark at 4°C for 3 days and grown in a vertical position under continuous light at 28°C. The _nom_ mutant was generated and characterised using standard techniques as detailed in the supplementary Materials and Methods. All experiments represent at least two independent replicates.

Cell division orientation
In plants, cell wall orientation reflects cell division orientation and those cell walls oriented at a 90° angle with the proximodistal axis were scored as transverse divisions; cell walls whose orientation differed more than a 10° angle from the transverse orientation were scored as oblique. Using ImageJ (NIH), cell walls were scored within a rectangular frame of 100 μm (length)×50 μm (height) drawn over confocal _z_-series and centred at 100 μm from the quiescent centre of 8 dpg root tips stained with Schiff and propidium iodide (PI).

Cell counting and meristem measurements
Epidermal and cortical cell numbers were counted on confocal, reconstructed transverse sections centred at 100 μm from the quiescent centre of 8 dpg root tips stained with Schiff-PI. The diameters of the meristems were measured on the same sections, excluding the lateral root cap tissue from the measurements. Root meristem size was measured on confocal, median, longitudinal sections of PI-stained roots using ImageJ software (NIH) as described previously (Dello Ioio et al., 2007).

Immunocytochemistry
α-tubulin immunostaining of 4 dpg seedlings was carried out using established techniques (Collings and Wateneys, 2005; Sauer et al., 2006) with some modifications as in supplementary Materials and Methods.

Microscopy and image processing

Confocal laser microscopy was performed with a Leica LCS SP5II microscope equipped with HyD detectors. The following wavelengths were used for fluorescence detection. Schiff-PI staining (Truernit et al., 2006): excitation, 488 nm and detection, 600-700 nm; GFP: excitation, 488 nm and detection, 493-550 nm; RFP: excitation, 561 nm and detection, 550-700 nm; DAPI: excitation, 405 nm and detection, 430-500 nm, as described in the supplementary Materials and Methods. Seedlings expressing the marker GFP-TUB6 were mounted in 50% MS liquid medium on slides and meristematic epidermal cells were imaged immediately.

Confocal images were processed with Image J64 software; reconstructed transverse sections were obtained by orthogonal projection of *z*-series collected at 0.4-0.5 µm intervals. Maximum intensity projections were done on *z*-series collected at 0.5 µm intervals for GFP-TUB6. Photoshop CS6 was used to prepare and pseudocolour the images for the figures. Images of longitudinal confocal sections and reconstructed transverse sections of PI-stained seedlings illustrating the organisation of tissues were inverted and their levels adjusted so that the PI staining, which outlines the profile of the cells, is in black.

Supplementary information

Supplementary information available online at
http://dev.biologists.org/lookup/suppl/doi:10.1242/dev.129502/-/DC1

References

Azimzadeh, J., Nacry, P., Christodoulidou, A., Drevensek, S., Camilleri, C., Amiour, N., Parcy, F., Pastuglia, M. and Bouchez, D. (2008). Arabidopsis TONNEAU1 proteins are essential for preprophase band formation and interact with centrin. *Plant Cell* **20**, 2146-2159.

Bichet, A., Desnos, T., Turner, S., Grandjean, O. and Hofte, H. (2001). BOTERO1 is required for normal orientation of cortical microtubules and anisotropic cell expansion in Arabidopsis. *Plant J.* **25**, 137-148.

Camilleri, C., Azimzadeh, J., Pastuglia, M., Bellini, C., Grandjean, O. and Bouchez, D. (2002). The Arabidopsis TONNEAU2 gene encodes a putative novel protein phosphatase 2A regulatory subunit essential for the control of the cortical cytoskeleton. *Plant Cell* **14**, 833-845.

Chan, J., Calder, G., Fox, S. and Lloyd, C. (2005). Localization of the microtubule end binding protein EB1 reveals alternative pathways of spindle development in Arabidopsis suspension cells. *Plant Cell* **17**, 1737-1748.

Dello Ioio, R., Linhares, F. S., Scacchi, E., Casamitjana-Martinez, E., Heidstra, R., Costantino, P. and Sabatini, S. (2007). Cytokinins determine Arabidopsis root-meristem size by controlling cell differentiation. *Curr. Biol.* **17**, 678-682.

Dolan, L., Janmaat, K., Willemsen, V., Linstead, P., Poethig, S., Roberts, K. and Scheres, B. (1993). Cellular organisation of the Arabidopsis thaliana root. *Development* **119**, 71-84.

Granger, C. L. and Cyr, R. J. (2001). Spatiotemporal relationships between growth and microtubule orientation as revealed in living root cells of *Arabidopsis thaliana* transformed with green-fluorescent-protein gene construct GFP-MBD. *Protoplasma* **216**, 201-214.

Gutierrez, R., Lindeboom, J. J., Paredez, A. R., Emons, A. M. and Ehrhardt, D. W. (2009). Arabidopsis cortical microtubules position cellulose synthase delivery to the plasma membrane and interact with cellulose synthase trafficking compartments. *Nat. Cell Biol.* **11**, 797-806.

Kirik, A., Ehrhardt, D. W. and Kirik, V. (2012). TONNEAU2/FASS regulates the geometry of microtubule nucleation and cortical array organization in interphase Arabidopsis cells. *Plant Cell* **24**, 1158-1170.

Marcus, A. I., Dixit, R. and Cyr, R. J. (2005). Narrowing of the preprophase microtubule band is not required for cell division plane determination in cultured plant cells. *Protoplasma* **226**, 169-174.

Masucci, J. D. and Schiefelbein, J. W. (1996). Hormones act downstream of TTG and GL2 to promote root hair outgrowth during epidermis development in the Arabidopsis root. *Plant Cell* **8**, 1505-1517.

Pickett-Heaps, J. D., Gunning, B. E. S., Brown, R. C., Lemmon, B. E. and Cleary, A. L. (1999). The cytoplast concept in dividing plant cells: Cytoplasmic domains and the evolution of spatially organized cell division. *Am. J. Bot.* **86**, 153-172.

Rasmussen, C. G., Humphries, J. A. and Smith, L. G. (2011). Determination of symmetric and asymmetric division planes in plant cells. *Annu. Rev. Plant Biol.* **62**, 387-409.

Rasmussen, C. G., Wright, A. J. and Müller, S. (2013). The role of the cytoskeleton and associated proteins in determination of the plant cell division plane. *Plant J.* **75**, 258-269.

Spinner, L., Gadeyne, A., Belcram, K., Goussot, M., Moison, M., Duroc, Y., Eeckhout, D., De Winne, N., Schaefer, E., Van De Slijke, E. et al. (2013). A protein phosphatase 2A complex spatially controls plant cell division. *Nat. Commun.* **4**, 1863.

Torres-Ruiz, R. A. and Jurgens, G. (1994). Mutations in the FASS gene uncouple pattern formation and morphogenesis in Arabidopsis development. *Development* **120**, 2967-2978.

Traas, J., Bellini, C., Nacry, P., Kronenberger, J., Bouchez, D. and Caboche, M. (1995). Normal differentiation patterns in plants lacking microtubular preprophase bands. *Nature* **375**, 676-677.

Truernit, E., Siemering, K. R., Hodge, S., Grbic, V. and Haseloff, J. (2006). A map of KNAT gene expression in the Arabidopsis root. *Plant Mol. Biol.* **60**, 1-20.
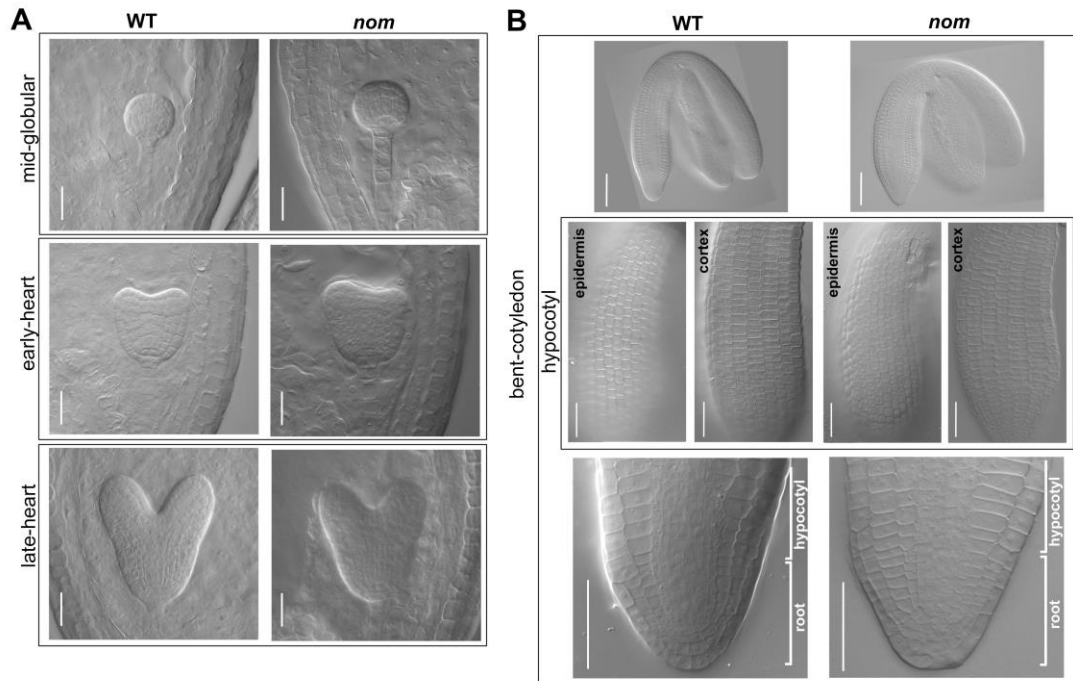
DEVELOPMENT

Figure S1. Division patterns along the root-hypocotyl axis are normal in *nom* embryos. Differential interference contrast (DIC) images of WT and *nom* embryos at different stages of development, stages were classified according to Jurgens, G. and Mayer, U. (Jurgens and Mayer, 1994), in (A) scale bars, 25 μm; in (B) at the top, whole seedlings, scale bars, 100 μm; in the centre, longitudinal view of the hypocotyl epidermis and cortex, note epidermal division patterns are unaltered in *nom*, scale bars, 50 μm; at the bottom, close ups of the root tips; scale bars, 50 μm.

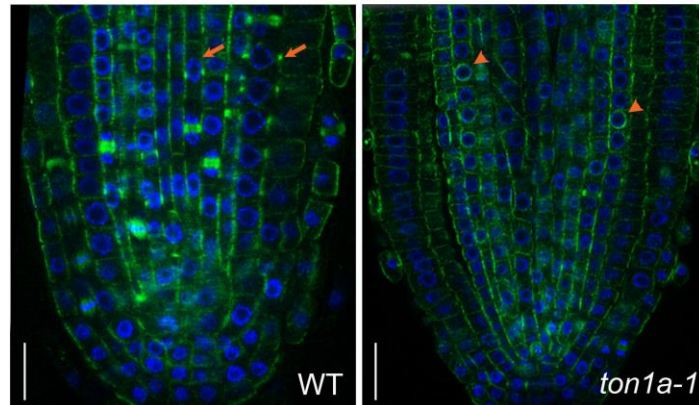**Figure S2. In the *ton1a-1* mutant, cells do not form PPBs.** Confocal longitudinal, single sections in the meristematic root tips of 4 dpg WT and *ton1a-1* seedlings immunostained with α-tubulin (green) and counterstained with DAPI (blue). PPB in the cortex and vasculature of WT (orange arrows); abundant MT surrounding the nucleus in the endodermis and pericycle of *ton1a-1* (orange arrowheads). Scale bars, 25 μm.
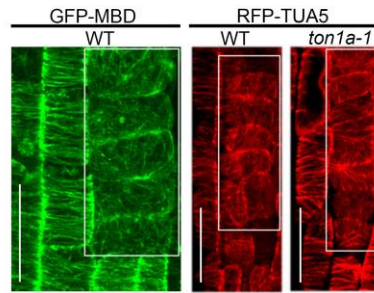
Figure S3. In root meristematic epidermal cells, interphase microtubules are not organised. Representative images of maximum intensity projections of confocal optical sections in the meristematic root epidermis of the microtubule marker line GFP-MBD (microtubule binding domain of MAP4) expressed in WT and of the microtubule marker line RFP-TUA5 expressed in WT and *ton1a-1* seeedlings. Note that epidermal cells (framed within white outlines) are present in the same projections as lateral root cap cells, which surround the epidermal tissue in the meristematic zone. In epidermal cells, microtubules are not organised, whilst in lateral root cap, microtubules have a prevalent transverse orientation; scale bars, 25 μm (for RFP-TUA5 WT n= 12 seedlings, *ton1a-1* n= 10 seedlings).

A

position (bp)	name	type	forward primer	reverse primer	in-del	TAIR accession
18001597	ALS	CAPS	GGCAACACATGTTCTTGGTG	ATCACAGGACAAGTCCCTCG		1945563
20017437	dc2	dCAPS	GTGCCGGAATCTCTAACCTG	GTGGTCTACACTAATTTATCACGAAT		
20358561	ind 1	INDEL	CGTATCACGAACCCCAAGAG	TGAATCACGGAAACATTCCA	TAGTAGAC/-	
20376570	ind 2	INDEL	CTTTCCGATCTTGATCTTCGTTAT	TCTCTCTCTCTCTCGTTTTTGACA	GAGAGAGG/-	
20387455	PUR5	CAPS	AAACCTTTCACTCCTCCTTTTTC	GATGTAGACCTTGCTGAAAA		1945637
20494897	ind 5	INDEL	TCACATGAAAAGTGTCAAACAACAC	GTCGTATGCAGTAGTTTTATTTCCA	CTAAA/-	
20762869	CIW20	SSLP	CATCGGCCTGAGTCAACT	CACCATAGCTTCTTCCTTTCTT		3433031
23168372	NGA112	SSLP	CTCTCCACCTCCTCCAGTACC	TAATCACGTGTATGCAGCTGC		1945516

B

ex1to8f	5'-ATGGATCTCAAGACTTTGGTCACT-3'
ex1to8r	5'-TCAATCTCTCCCTTCTTCTTCATT-3'
05ex1to7f	5'-TGATGGATCTCAAGACCTTAGTCA-3'
05ex1to7r	5'-CTTTCCCTTCTTCTTCTTCACTTG-3'
ex2-3to7f	5'-GCTTCTCCTTCAGGAAGGTTACTA-3'
ex2-3to7r	5'-TAGACAACCCGGCTCTTCTATC-3'
EF1a-f	5'-ATGCCCCAGGACATCGTGATT-3'
EF1a-r	5'-TTGGCGGCACCCTTAGCTGGA-3'
CL001f	5'-ATTGGTGAAGAAAAGGAGTTTCAA-3'
CL001r	5'-TGACGGATCAGATCAAAATAACAG-3'
Site2-1f	5'-AAGCTTCATGCTTCTCCTCCAG-3'
Site2-1r	5'-TCCACGAATCTTTTGGCTTT-3'
8474	5'-ATAATAACGCTGCGGACATCTACATTTT-3'
NF09	5'-GAAGCTGAAATGTTTATCCAAAGC-3'
3144	5'-GTGGATTGATGTGATATCTCC-3'
DC48	5'-CAACTTGCTTTGTTTTCATTTCAA-3'

Supplementary Table S1. Sequences of primer pairs. (A) Primer pairs used for mapping and their genomic position on chromosome III. (B) Primer pairs used in cloning, genotyping and RT-PCR experiments.

Supplementary Materials and Methods

Mutagenesis

The *nom* mutant was generated by ethyl methanesulfonate (EMS) mutagenesis of the *GL2::GUS* line (WS ecotype). 0.48 g of dried seeds were imbibed and vernalised in water for four days and treated in 0.3% (v/v) EMS for 8 hours, thoroughly rinsed with water and sown on soil. Pools of 4 day-post-germination (dpg) M2 seedlings were pre-screened for those seedlings with normal root growth that, under the compound microscope, displayed defects in the orientation of cell division in the root meristematic epidermis. Candidate pools were re-screened by cutting off the primary root tip and analysing the phenotype of the meristematic epidermis, once identified the tips with mutant phenotypes, their corresponding seedlings were traced back and moved onto soil.

Segregation analysis

Upon outcrossing *nom* to Col-0, all F1 seedlings were normal and displayed a wild type (WT) organisation of the root meristematic epidermis. The F1 plants were left to self–fertilise and the meristematic epidermis of 539 F2 seedlings was analysed, 430 displayed a WT phenotype and 109 a *nom* phenotype, so 20.22% displayed the mutant phenotype. These values are slightly lower than the 25% expected for a recessive mutation, as the chi test on our sample gives a $\chi^2=6.31$, which exceeds for a p=0.05 that of $\chi^2 =3.84$ and they are likely due to mis-scoring under the compound microscope as the mutant phenotype is subtle. In fact, we did not observe embryo lethality or failure of the seedlings to germinate and in the subsequent phenotypic analyses with the confocal microscope of genotyped, homozygous *nom/ton1a-1* mutant meristems we always observed the *nom* phenotype behaving as fully penetrant and we can confidently conclude that the *nom* phenotype results from a recessive mutation.

Mapping and complementation

Homozygous *nom* plants in the WS background were crossed to ecotype Col-0. In the F2 *nom* homozygous mutant seedlings were selected for their meristematic epidermal phenotype under the compound microscope and their DNA was isolated. We initially mapped *nom* to chromosome 3, between the markers ALS and NGA112; the other markers tested, which were evenly distributed through the five chromosomes, gave recombinant frequencies close to 50%, indicating independent segregation. We then fine mapped the mutation to a 10,885bp interval by screening 884 F2 seedlings

displaying the *nom* mutant phenotype using a PCR-based approach with SSLP, dCAPS and Indel markers selected from the TAIR collection and designed using TAIR (http://www.arabidopsis.org) and the EnsemblPlants (http://plants.ensembl.org) for essential genome information. Primer pairs sequences can be found in Supplementary Table S1.We identified one recombinant for the ind2 marker and one recombinant for the PUR5 marker and we then comparatively sequenced candidate genes in this interval from the parental transgenic *GL2::GUS* line and the *nom* allele. Two point mutations were identified within the sequence of the *TON1a* gene in *nom*, one inside intron 1 and one in the canonical GT acceptor splice site of intron 2 (Fig. 2A).

We confirmed the mapping results by complementation and expressed, in the *nom* mutant background, a 5.6Kb genomic construct encompassing the entire *TON1a* gene and including 3Kb upstream the start and 1Kb downstream the stop codons of *TON1a*. About 120 T2 seedling roots for each of 12 independent BASTA resistant T1 transformants were examined and found to segregate WT roots with no defects in cell division orientation in the root meristematic epidermis. Root tips of T2 populations were phenotyped under the compound microscope to detect and score plants with *nom* and WT phenotype meristematic epidermis. To further verify the complementation, seedlings from a chosen segregating T2 line where subjected to confocal analysis (Fig. 2B, C) and genotyped to ascertain that those root tips with a WT phenotype were *nom* homozygous mutant at the endogenous locus.

Plant vectors and transformation

The construct to complement the *nom* mutation was generated by amplifying 5.6Kb of genomic DNA (Col-0 ecotype) from JAty 76F24 clone with primers CL001F+R using Phusion Taq (Thermo Scientific). The genomic fragment was subcloned into pGEM-T (Promega), released with NotI and cloned into the binary vector pMLBART/pW3. The pMLBART/pW3 carries the bialophos resistance gene (BAR) that encodes the phosphinotricin acetyl transferase and confers to transformed plants resistance to the herbicide ammonium-glufosinate, commercially known as BASTA (Bayer). Constructs were confirmed by sequencing. The Agrobacterium strain GV3101 was used to transform homozygous *nom* mutant plants by the floral dip method (Clough and Bent, 1998).

Microscopy

Z-series of root meristems stained with Schiff-PI method were collected at intervals of 0.4-0.5 μm with an objective HC PL APO 20x/0.70 IMM CORR CS at a 400Hz scan speed on Bidirectional mode. Seedlings from GFP expressing lines were counterstained with 0.1-0.5 mg/ml propidium iodide (PI) solution (Sigma-Aldrich). Confocal images of seedlings expressing RFP-TUA5 were collected at intervals of 0.3-0.5 μm with HCX PL APO 40x/1.25-0.75 oil CS or HCK PL APO 63x/1.20 W CORR CS objectives, Airy set on 1 and scan speed between 200-400Hz. For double-stained samples, z-series were always collected in sequential mode.

Images of resin embedded and sectioned root meristem, prepared according to Dolan et al. (Dolan et al., 1993), were captured with a Leica DM 6000 microscope.

Differential interference contrast (DIC) images of embryos cleared with a chloral hydrate solution (glycerol, chloral hydrate and water in a ratio of 1:8:3), were captured with a Leica DM 6000 microscope.

Marker gene analysis and PCR based genotyping

The T-DNA insertion lines were confirmed by PCR-genotyping and sequencing. Transgenic marker lines in the *ton1a-1* mutant background were generated by genetic crossing. Homozygous seedlings for *ton1a-1* and expressing the transgene markers were identified from segregating F2 population based on marker fluorescence, phenotype and genotype, then reconfirmed in the F3 generation and analysed. WT siblings were used as controls in all the experiments.

The *ton1a-1* mutant allele was genotyped using primers Site2-1F and Site2-1R that generate a dCAP marker with BstNI enzyme (CCWGG) that cuts the WT but not the *ton1a-1* allele. The *ton1a-2* allele was genotyped with the primer pair 3144 and DC48 and the *ton1a-3* allele with the primer pair 8474 and NF09. Primer sequences can be found in Supplementary Table S1B.

Expression analysis

RNA was extracted using the RNeasy Plant mini kit (Qiagen), and treated with DNnase I (Roche) to remove DNA contamination. cDNA was obtained and amplified with the different primer pairs with the One Step RT-PCR kit (Qiagen). For each sample, 350 ng of total RNA were used for 35 cycles in a single step RT-PCR reaction.

Immunolabelling

Seedlings were fixed for 1 hour in 4% (w/v) paraformaldehyde prepared in PEM (50mM Pipes, 10mM EGTA, 5mM MgSo4, pH 7) supplemented with 0.05% Triton X-100. For the first 30 minutes seedlings were fixed under mild vacuum. After fixation seedlings were rinsed four times in PEM for 30 minutes, transferred onto slides with wide shallow wells and digested for 15 minutes at room temperature in a cell wall enzyme mix of 1% driselase from *Basidiomycetes* sp. (Sigma-Aldrich), 2% cellulase from *Trichoderma viride* (Sigma-Aldrich), 0.1% pectolyase from *Aspergillus japonicus* (Sigma-Aldrich) in PEM, rinsed again four times in PEM for 30 minutes. Samples were further permeabilized for 40 minutes in PEM containing 3% IGEPAL (Sigma-Aldrich) and 10% DMSO, rinsed for 15 minutes in PEM and 15 minutes in PBS (137mM NaCl, 2.7mM KCl, 7mM Na_2HPO_4, 3mM NaH_2PO_4). An incubation of one hour in a blocking solution of 3%BSA, 0.05% Trition X100 in PBS, was followed by O/N incubation at 4°C with monoclonal anti-α-tubulin antibody produced in mouse, clone B-5-1-2 (Sigma-Aldrich Cat. No. T5168), and diluted 1:150 in blocking solution. Seedlings were rinsed six times in freshly made blocking solution for 1 hour and incubated for 2 hours with a secondary antibody Alexa Fluor 488 goat anti-mouse IgG (Invitrogen Cat. N. A-11001) diluted 1:300 in blocking solution, then rinsed three times in blocking solution and three times in PBS for a total of 1 hour. Samples were counterstained with 1 μg/ml of 4′,6-diamidino-2-phenylindole dihydrochloride (DAPI) in H_2O, washed twice in H_2O and mounted in Vectashield (Vector Laboratories), after carefully removing excess water.

References

Clough, S. J. and Bent, A. F. (1998). Floral dip: a simplified method for Agrobacterium-mediated transformation of Arabidopsis thaliana. *Plant J* **16**, 735-43.

Dolan, L., Janmaat, K., Willemsen, V., Linstead, P., Poethig, S., Roberts, K. and Scheres, B. (1993). Cellular organisation of the Arabidopsis thaliana root. *Development* **119**, 71-84.

Jurgens, G. and Mayer, U. (1994). Arabidopsis. *In EMBRYOS. Colour atlas of development (ed. J. Brand). London: Wolfe publications.*, 7-21.